Polymer Chemistry

Accepted Manuscript

ROYAL SOCIETY OF CHEMISTRY

www.rsc.org/polymers

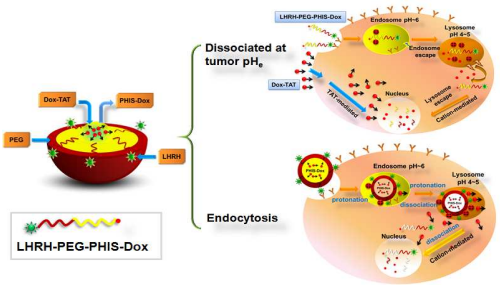

Dox in LHRH-PEG-PHIS-Dox/Dox-TAT system could be transported into tumor cells by two pathways: LHRH receptor-mediated endocytosis and TAT-mediated nonendocytotic process.

Multifunctional pH-sensitive Micelles for Tumor-Specific Uptake and Cellular Delivery

Tiehong Yang[a‡], Fei Li[a‡], Haitao Zhang [a], Li Fan[a], Youbei Qiao[a], Guangguo Tan[a], Haifei Zhang[b], Hong Wu[a*]

Received (in XXX, XXX) Xth XXXXXXXXX 20XX, Accepted Xth XXXXXXXXX 20XX
DOI:

The distinct ability of cell-penetrating peptides (CPPs) has lead to development of novel drug delivery methods in human cells for therapeutic purposes. The lack of specific selectivity is a main obstacle of CPPs. A novel delivery method based on acid-sensitive micelles using for the introduction and protection of TAT was developed in this study. Doxorubicin-TAT conjugate (Dox-TAT) was loaded in the luteinizing hormone-releasing hormone modified poly (ethylene glycol)-poly (L-histidine)-doxorubicin (LHRH-PEG-PHIS-Dox) micelle. Dox was chemically conjugated to the polymer backbone for not only improving the stability of the micelles, but also increasing drug loading efficiency of the micelle. These micelles could dissociate responding tumor extracellular pH_e and release Dox-TAT to pass directly through the cell membrane to the cytosol of multidrug resistant cancer cells. The undissociated micelles could also be actively internalized into the cells by receptor-mediated endocytosis, resulting in high cytotoxicity. LHRH-PEG-PHIS-Dox/Dox-TAT showed highest antitumor effects among four treatment groups *in vitro* and *vivo* and showed no remarkable on body weight when compared with control. This skillfully designed system combined the double functions of targeted delivery and TAT-mediated efficient entry, which could increase antitumor activity even in drug resistant tumor cells.

Introduction

Multifunctional drug delivery systems including liposomes, polymeric micelles, and polymer-drug conjugates have been developed for cancer chemotherapy. Although many drug delivery systems have shown good tumor active target efficiency via specific ligands and delivered drugs to tumor cell surface, they could not provide sufficiently high intracellular drug concentration because of the weak binding affinity of carriers to the target cells.[1] Moreover, most targeting therapeutic systems rely on the receptor-mediated endocytotic pathway for internalization into cells, which leads to the entrapment and degradation of transported biomolecules in lysosomes.[2]

In an attempt to avoid these limitations, cell-penetrating peptides (CPPs) were introduced to the drug delivery system.[3-6] Candidate drug conjugation to CPPs represents a promising tool to overcome cell and tissue barriers. One of the most promising and most studied CPPs is the HIV-1 transactivator of transcription peptide (TAT). TAT can be efficiently linked to different therapeutic molecules, including small molecules and antibodies, peptides, liposomes, nanoparticles, and so on.[7] It could avoid endocytosis pathway and take the cargo directly into the cells with an energy-independent way, even for drug-resistant tumor cells.[8-13] It has been reported that coupling Dox directly to TAT conjugate (Dox-TAT) could overcome drug resistance and greatly enhance Dox intracellular delivery. The IC_{50} of Dox-TAT conjugate was 8-10 times less than that of free doxorubicin.[14] However, the TAT peptide is a non-specific cell penetrating peptide, the main obstacle that still remains unresolved is the lack of selectivity. To this end, shielding/deshielding approach for delivering TAT was developed.[15-17] Within this paradigm to control CPPs delivery, three types of controlled strategies have been investigated: (1) "charge"controlled delivery of CPPs by recovering their cationic nature from a charge-blocked state; (2) "steric hindrance" controlled delivery of CPPs by exposing their cell-penetrating function from a hidden state; and (3) "density" controlled delivery of CPPs by increasing their local density at a target site.[18] These methods usually involve tedious procedures of chemical synthesis and purification, prompting us to develop a more universal delivery and entry strategy for solid tumors by introducing a non-specific TAT peptide to drugs or drug carriers.

The extracellular pH (pH_e) in most solid tumors is lower (pH 6.5-7.2) than that in normal tissues (pH 7.4). After the drug carriers are taken up by cells there is still pH variation at different stages. So, the development of drug carriers that respond to pH_e of solid tumors or endosomal pH (5.0-6.5) is a favorable strategy to trigger the extensive release of anticancer drugs and decrease side effects in normal tissues.[19] Wang et al. [20] reported a smart drug delivery system contained two pH-sensitive groups: citraconic amide and hydrazone linker. Citraconic amide group can enhance tumor therapy efficiency by the extracellular pH-sensitive charge-conversion property. Hydrazone linker between polymer and drug can cleave efficiently in the intracellular pH environment. The resulting conjugate showed dual-pH sensitive properties: extracellular pH-triggered

[a] Department of Pharmaceutical Analysis, School of Pharmacy, Fourth Military Medical University, Xi'an 710032, China
[b] Department of Chemistry, University of Liverpool, LiverpoolL69 7ZD, United Kingdom
‡ These authors contributed equally to this work.
* Corresponding author: School of Pharmacy, Fourth Military Medical University, Xi'an 710032, China
Tel: +86 29 84776823; Fax: +86 29 84776823. *E-mail address:* wuhong@fmmu.edu.cn (H. Wu)

enhanced tumor targeting and intracellular pH-triggered drug release. In addition, a novel pH-sensitive polymeric mixed micelle composed of PHIS-PEG (polyethylene glycol-coupled poly-L-histidine) and DSPE-PEG (1,2-distearoyl-sn-glycero-3-phosphoethanolamine-polyethylene glycol) was also developed. The mixed micelles were stable at tumor pH_e and could be endocytosed as intact micelle. When pH drops to around 5.5 in endosome, a destabilization of micelles is observed caused by phase separation in the micelle core and dissociation of the ionized PHIS-PEG molecules.[21] Furthermore, the pH-sensitive mixed micelles system has been demonstrated to be a promising approach for overcoming the multidrug resistance.[22] pH-Sensitive drug carrier could also be used to protect CPP by differentiating the intrinsic differences between solid tumors and the surrounding normal tissues.[23] Poly-L-histidine (PHIS) is an excellent pH-sensitive candidate.[24] The imidazole ring of PHIS has an electron lone pair on the unsaturated nitrogen that endows PHIS with an amphoteric nature by protonation–deprotonation. The fusogenic activity of PHIS could disrupt the enveloped membrane of acidic subcellular compartments such as endosomes, resulting in drugs reaching the cytosol to enhance the delivery efficiency.[2] Since pH-sensitivity of PHIS could be adjusted by structural modification, PHIS-based micelles have great potential as an acid triggering tumor-killing platform.

Since the core of the micelles constituted by PHIS solely is less stable because of the pH ultrasensitivity of the PHIS segments, PHIS was combined with more hydrophobic segments[25] or mixed with other copolymers[21] to improve micelle stability. In this research, hydrophobic Dox was chemically conjugated to the polymer backbone (LHRH-PEG-PHIS) not only to stabilize the core of micelles, but also to increase drug loading efficiency of the micelles. Then the luteinizing hormone-releasing hormone modified LHRH-PEG-PHIS-Dox micelles were prepared for Dox-TAT delivery. The micelles could dissociate responding tumor extracellular pH_e and release Dox-TAT. Then the released Dox-TAT could pass directly through the cell membrane, resulting in high cytotoxicity. At the same time, the undissociated micelles could also be actively internalized into the cells by receptor-mediated endocytosis (Figure 1). Therefore, LHRH-PEG-PHIS-Dox/Dox-TAT micelles would combine the advantages of both LHRH-mediated and TAT-mediated cargo delivery systems, and facilitate cellular uptake of drug molecular as far as possible. The pH sensitivity and drug release characteristics of the LHRH-PEG-PHIS-Dox micelles were also investigated, and the antitumor activity *in vitro* and *vivo* and cellular uptake were evaluated in LHRH receptor-positive Dox-resistant A2780 human ovarian ($A2780/Dox^R$) cancer cells.

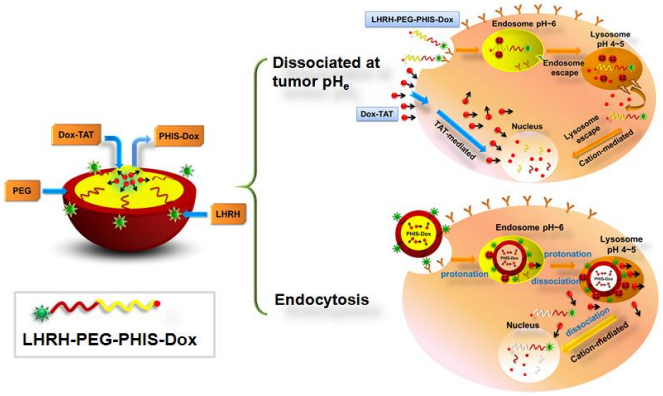

Fig 1. The pathways of LHRH-PEG-PHIS-Dox/Dox-TAT micelles entering into tumor cells.

Materials and methods

Materials

Poly (L-histidine) (PHIS) with a number average molecular weight of 15,000 Da (as verified by gel-permeation chromatography) was purchased from Sigma Chemical Co. NHS-polyethylene glycol-COOH (NHS-PEG-COOH; Mn 5,000) was purchased from Nanocs Inc. (NewYork, USA). 1-ethyl-3-(3-dimethylaminopropyl) carbodiimide hydrochloride (EDC·HCl), N-hydroxysuccinimide (NHS) and Doxorubicin hydrochloride (Dox·HCl), 3-(4,5-dimethylthiazol-2-yl)-2,5-diphenyl tetrazolium bromide (MTT), dulbecco's modified eagel medium (DMEM), fetal bovine serum (FBS) and Trypsin-EDTA were obtained from Sigma Chemical Co. (USA). LHRH analog (Gln-His-Trp-Ser-Tyr-DLys-Leu-Arg-Pro-NH-Et) and Doxorubicin-TAT conjugate (Dox-TAT) were purchased from TASH Biotechnology Co. Ltd. (Shanghai, China). Dimethyl formamide (DMF), dimethyl sulphoxide (DMSO) and triethylamine (TEA) were obtained from Baotelai Chemicals (Xi'an, China). All solvents were thoroughly dried and distilled before use. All aqueous buffers were prepared by deionized water produced from Milli-Q Synthesis.

Synthesis of LHRH-PEG-COOH

120 mg (0.10 mmoL) of LHRH peptide and 250 mg (0.05 mmoL) NHS-PEG-COOH in 20 mL of DMF reacted at room temperature for 24 h. Then the reaction mixture was dialyzed for 48 h against deionized water using a dialysis tube

(molecular weight cutoff: 3,500) to remove the unreacted LHRH and reagents. The deionized water was changed every 2 h. The solution was lyophilized and the white solid was obtained with the yield of 86%.

Synthesis of PHIS-Dox

PHIS (0.01 mmoL) reacted with NHS (0.015 mmoL) and EDC (0.013 mmoL) in 20 mL of deionized water at pH 6.0 to give activated NHS-PHIS solution. The Dox base solution was obtained by trearment of Dox·HCl (0.02 mmoL) with 2.0 equivalents of triethylamine (TEA) in 10mL of DMSO for 12 h in the dark. Subsequently, Dox base solution was added to the NHS-PHIS solution and the mixture was stirred at room temperature for 24 h. The product was dialyzed in DMSO using dialysis membrane with the molecular weight cutoff of 10,000 for one day to remove excess reagents and unconjugated Dox, and further dialyzed against deionized water for two days to remove DMSO. The resulting solution was freeze-dried and the pink powder was obtained in 75% yield.

Synthesis of LHRH-PEG-PHIS-Dox

The carboxylic groups of LHRH-PEG-COOH were activated using the same method as described above. Briefly, 0.02 mmoL LHRH-PEG-COOH was reacted with EDC·HCl and NHS in DMSO at molar ratio of 1:1.3:1.5 for 12 h at 25 ℃. Then a solution of PHIS-Dox (0.01 mmoL) in deionized water at pH 6.0 was added slowly. The mixture was stirred at room temperature for 24 h. After the reaction was completed, the solution was dialyzed against deionized water successively using dialysis membrane with the molecular weight cutoff of 10,000 for 48 h. After filtration through a 0.45 μm filter, the solution was lyophilized and the powder was obtained with a yield of 72%.

Structural analysis of synthesized polymers

The polymers were dissolved in CF_3COOD (10 mg/mL). The ^{1}H-NMR spectrum was recorded at room temperature with a Bruker Avance 500 MHz spectrometer (Germany), and the chemical shifts were expressed in ppm relative to the resonance of the internal standard, tetramethyl silane (TMS). Molecular weights of the polymers were determined by a GPC with triple detectors, including a refractive index detector, a viscometer detector and a light scattering detector (Viscotek, USA). Phosphate buffer solution (100 mM, pH 6.0) was used as a mobile phase at a flow rate of 1.0 mL/min, and a column thermostat was maintained at 25 ℃. Molecular weight calibration was performed with the polyethylene glycol standards (Mp 1k-30k) from Fluka.

Acid-base titration of LHRH-PEG-PHIS-Dox

For measurement of pK_b value, LHRH-PEG-PHIS-Dox (1.5 mg) was dissolved in 4.0 mL deionized water and adjusted to pH 12 with 1 mol/L NaOH, and titrated by stepwise addition of 0.1 mol/L HCl to obtain the titration profile. The average value obtained from triplicate titrations was plotted.

Conjugate efficiency of Dox

To determine the conjugate efficiency, 2.0 mg PHIS-Dox and LHRH-PEG-PHIS-Dox were added to 20 mL pH 5.0 phosphate buffer solution containing 0.02% Tween 20 at 50 ℃ with magnetic stirring at 200 rpm for 8h, respectively. The amount of conjugated Dox was measured by FP-6000 fluorescence spectrophotometer (Jasco, Japan; ex: 485 nm; em: 595 nm) and then compared with a standard curve of Dox generated from the same solvent with Dox concentrations varying from 0 to 100 μg/mL.

Preparation of LHRH-PEG-PHIS-Dox micelles

LHRH-PEG-PHIS-Dox micelles were prepared by the improved dialysis method. Briefly, LHRH-PEG-PHIS-Dox was first dissolved in DMF with the initial copolymer concentration at 3.0 mg/mL. Distilled water was then added to the polymer solution at a rate of 1 drop every 5-10 s with vigorous stirring until water content was up to 20% of the original solution by volume. Next, the mixed solution was sonicated at 100W for 10min and further dialyzed (Molecular weight cut-off, MWCO 3500) against deionized water for 12 h to remove organic solvents. The deionized water was exchanged at an interval of 2 h. The yield (wt %) of nanoparticles was calculated by weighing the freeze-dried micelle powder.

Dox-TAT and Dox were employed as drug models respectively. The preparation procedure of drug-loaded micelles was similar to that of the micelles without being drug-loaded. Dox-TAT and LHRH-PEG-PHIS-Dox polymer were first dissolved in DMF. The concentrations of Dox-TAT and polymer were 0.5 mg/mL and 3.0 mg/mL, respectively. Distilled water was then added to form pre-structure micelle. Next, the mixed solution was sonicated at 4 ℃ for 10min and further dialyzed against deionized water for 12h to remove organic solvents. The distilled water was exchanged at an interval of 2 h. LHRH-PEG-PHIS-Dox/Dox micelles were prepared by the same method.

Critical Micellar Concentration (CMC) measurement

The freeze-dried micelle sample was dispersed in pH7.4 phosphate buffer solution (0.02M, ionic strength 0.15). A stock solution of pyrene (6.0×10^{-2} M) in acetone was prepared and stored at 5 ℃ until use. In order to measure the steady-state fluorescence spectra, this solution was added to distilled water, yielding a pyrene concentration of 12.0×10^{-7} M. The solution

was then distilled under vacuum at 60 ℃ for 1 h to remove acetone. The acetone-free pyrene solution was mixed with the solutions containing LHRH-PEG-PHIS-Dox polymer at a range of concentrations from 1×10^{-4} mg/mL to 1.0 mg/mL. The final pyrene concentration in each sample solution was 6.0×10^{-7} M, which is nearly equal to its solubility in water at 25 ℃. The fluorescence measurement was performed using a FP-6000 fluorescence spectrophotometer. The CMC was estimated by the intensity ratio measurement of the third and the first highest energy bands in the emission spectra profile against the log of the micelle concentration. The CMC of LHRH-PEG-PHIS-Dox polymer was determined from the crossover point at low polymer concentration in this plot.[26]

Transmission electron microscope (TEM)

The morphologies of the nanoparticles were observed under a JEM-2010 microscope (Japan) with an electron kinetic energy of 300 kev. The samples were placed onto a carbon-coated copper grid followed by drying at room temperature.

Dynamic light scattering (DLS)

The particle size and zeta potential of the self-assembled micelles were measured by a Malvern Zetasizer, MODEL NANO ZS (Malvern Instruments Limited, UK). Water dispersion (1 mL) of micelles was analyzed in a polystyrene cell at 25 ℃, using a He-Ne laser -wavelength of 633 nm and a detector angle of 90 º. The polymeric micelles were exposed to different pH values for 24 h before measurement of the particle size and zeta potential.

Drug loading efficiency

To quantify the amount of Dox-TAT encapsulated, a given amount of freeze dried micelles were completely dissolved in pH 5.0 phosphate buffer solution containing 0.02% Tween 20 at 50 ℃ with magnetic stirring at 200 rpm for 8h. This solution was analyzed by fluorescence spectrophotometer at 485 nm excitation and 595 nm emissions. Compared with a standard curve, the total Dox concentration was calculated. The loading efficiency of Dox-TAT was calculated by the following equation:

$$\text{Loading efficiency (\%)} = \frac{(N_{\text{Dox in micelles}} - N_{\text{Dox in conjugates}}) \times M_{\text{Dox-TAT}}}{\text{Mass of drug-loaded micelles}} \times 100 \quad (1)$$

$N_{\text{Dox in micelles}}$: Molar of Dox in micelles
$N_{\text{Dox in conjugate}}$: Molar of Dox in LHRH-PEG-PHIS-Dox conjugate
$M_{\text{Dox-TAT}}$: Molar mass of Dox-TAT

The loading efficiency of LHRH-PEG-PHIS-Dox/Dox micelles was calculated by the following equation:

$$\text{Loading efficiency (\%)} = \frac{(N_{\text{Dox in micelles}} - N_{\text{Dox in conjugates}}) \times M_{\text{Dox}}}{\text{Mass of drug-loaded micelles}} \times 100 \quad (2)$$

M_{Dox}: Molar mass of Dox

In vitro drug release studies

10mg of drug-loaded micelles was dialyzed against 50 mL of PBS (molecular weight cutoff, 3,000) containing 0.02% Tween 20 at different pH (pH 5.0, 6.8 or 7.4) at 37 ℃ with horizontal shaking (100 rpm). At hourly intervals, a 1 mL sample was taken out from the release medium and the same volume of PBS at the same pH was added to the release medium. Fluorescence intensity was measured at λ_{ex}485 nm and the total Dox concentration was determined.

Cell culture

LHRH receptor-positive Dox-resistant ovarian carcinoma A2780 (A2780/Dox^R) cell line was provided kindly by the department of gynaecology and obstetrics, Xijing Hospital Xi'an, China. The cells were cultured in DMEM medium supplemented with 10% fetal bovine serum and antibiotics, in a humidified incubator with 5% CO_2 at 37 ℃.

In vitro cytotoxicity assay

In order to compare the cytotoxicity of different drug delivery systems, A2780/Dox^R cells were seeded into 96-well plate (5×10^4 cells/well) and incubated for 24 h. Then the medium was replaced by LHRH-PEG-PHIS-Dox/Dox-TAT, LHRH-PEG-PHIS-Dox/Dox, LHRH-PEG-PHIS-Dox，Dox-TAT or Dox in DMEM medium with different pH (pH 6.8 or 7.4). The concentration of LHRH-PEG-PHIS-Dox/Dox-TAT or Dox-TAT was 3.8 μg/mL of Dox, and that of LHRH-PEG-PHIS-Dox/Dox, LHRH-PEG-PHIS-Dox or Dox were 14.7 μg/mL of Dox. The cells were incubated for another 48 h before replacing the medium within each well with 180 μL of fresh DMEM medium and 20 μL of MTT solution (5 mg/mL). After incubation for another 4 h, 200 μL of DMSO was added to dissolve the formazan crystals formed. And the absorbance at 480 nm of the resulting solution was measured using a microplate reader (GENios, Tecan, Switzerland). The inhibitory rate was calculated as follows:

Inhibitory rate (%) = $(A_{\text{control}}-A_{\text{sample}})/A_{\text{control}}\times100\%$. (3)

Flow Cytometry study

A2780/Dox^R cells were seeded into 12-well plate (2×10^5 cells/well). When the cells reached about 80% confluence, the medium was replaced by 1.0 mL of LHRH-PEG-PHIS-Dox/Dox-TAT, LHRH-PEG-PHIS-Dox/Dox, LHRH-PEG-PHIS-Dox or Dox in DMEM with different pH (6.8, 7.4) and incubated in a incubator with 5% CO_2 at 37 ℃ for one hour. Then the cells were washed three times with PBS (pH 7.4) and detached by 0.02% (w/v) EDTA-0.025% (w/v) trypsin solution. The cells were collected and resuspended in 0.5 mL of PBS and the uptake was analyzed based on the Dox fluorescence using a flow cytometer (BD FACSAria). Cells without Dox treatment were used as a negative control.

Confocal laser scanning microscopy study

The cellular uptake of micelles was further studied using confocal laser scanning microscopy. A2780/Dox^R cells were grown on coverslips for 24 h in a 12-well plate. Then the DMEM medium with serum was replaced by 1.0 mL of LHRH-PEG-PHIS-Dox/Dox-TAT or LHRH-PEG-PHIS-Dox in DMEM medium without serum at pH 6.8, at the equivalent concentration of Dox. The cells were cultured at 37 ℃ or 4 ℃ for 1 h, the cell-plated coverslips were washed 3 times with PBS (pH 7.4) and followed by cell nuclei staining with Hoechst 33342 for 20 min. After the cells were washed with PBS, fluorescent images were analyzed by a confocal laser scanning microscopy (Olympus FV1000).

Anti-tumor activity in vivo

The Committee on Animal Experimentation of the Fourth Military Medical University approved all the animal experiments. A2780/Dox^R cells (2×10^6) were implanted subcutaneously into the right flank of the nude female mice. Mice were divided randomly into five groups; the first 4 groups were treated with LHRH-PEG-PHIS-Dox/Dox-TAT, LHRH-PEG-PHIS-Dox/Dox, LHRH-PEG-PHIS-Dox micelles and plain drug (Dox) solution, respectively at a dose having equivalent amount of Dox (5 mg/kg body weight) after sufficient growth of tumor (approximately to a volume of 100 mm^3) and the fourth group served as control group. All four formulations (plain drug solution, LHRH-PEG-PHIS-Dox/Dox-TAT, LHRH-PEG-PHIS-Dox/Dox and LHRH-PEG-PHIS-Dox) in isotonic PBS (pH 7.4) solution were injected to animals at 0th and 7th day via tail vein. During the experiment the major and minor axes of tumor were measured by means of vernier caliper every other day. Acute toxicity was checked by monitoring the body weight changes. Volume of tumor (V) was determined using the following formula: $V = 0.5\times a\times b^2$, where a is the largest diameter and b is the smallest diameter.

Statistical analysis

Statistical analysis was conducted by using the one-way ANOVA with Student's *t*-test with $P < 0.05$ as significant difference.

Results and discussion

Characterization of LHRH-PEG-PHIS-Dox polymer

The overall synthetic route of LHRH-PEG-PHIS-Dox was represented in Figure 2. All conjugations between the amino group and the carboxyl group were conducted via the conventional carbodiimide reaction. To reduce the side products and avoid tedious procedures of purification, LHRH-PEG-COOH was synthesized from the reaction between NHS-PEG-COOH and 2-fold excess of LHRH (Figure 2A). The unreacted LHRH and reagents were easily removed by dialysis. Similarly, excessive Dox was introduced to achieve complete reaction with PHIS (Figure 2B). LHRH-PEG-COOH was coupled with PHIS-Dox using amide linkages. It was also convenient to separate Dox from the large molecular mass conjugate PHIS-Dox by dialysis. The unreacted PHIS or PHIS-Dox would precipitate in the dialysis process, and was filtered out. LHRH-PEG-COOH, PHIS-Dox and LHRH-PEG-PHIS-Dox were synthesised successfully and confirmed by ^{1}H-NMR spectra (Figure 3). As shown in Figure 3A, the peak at 3.63 ppm, corresponding to PEG blocks (peak a), the two peaks at 2.42 and 4.28 ppm were attributed to the methylene protons in LHRH-PEG-COOH (peak b and c). Chemical shifts from 6.72 ppm to 7.50 ppm were attributed to protons on the LHRH peptide (peak d). These data indicated that the target products were synthesized successfully. Figure 3B was the spectrum of PHIS-Dox. δ 2.9 (–CH_2–, g), δ 6.88 (–C=CH–N, h) and δ 8.01 (–N=CH–, i) were the striking features of poly (L-histidine). The two peaks at 11.56 (f) and 12.44 (g) ppm were assigned to protons of two hydroxyl groups of Dox structure, indicating successful preparation of PHIS-Dox. Figure 3C is the spectrum of LHRH-PEG-PHIS-Dox. Chemical shifts from poly (L-histidine), Dox and PEG were visible in the spectrum, δ 6.72-7.50 (protons on the LHRH peptide) shown in Figure 3B were disappeared in Figure 3C. This could be due to PHIS peaks that were strong enough to merge with some peaks of LHRH peptide.

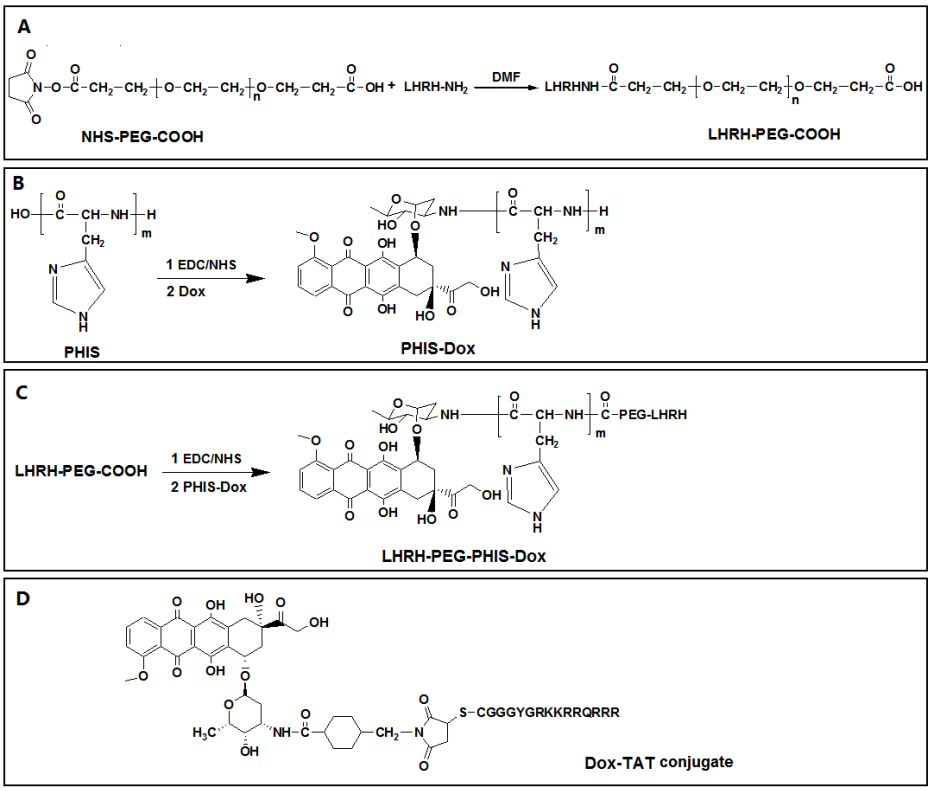

Fig 2. Synthetic route of LHRH-PEG-PHIS-Dox.

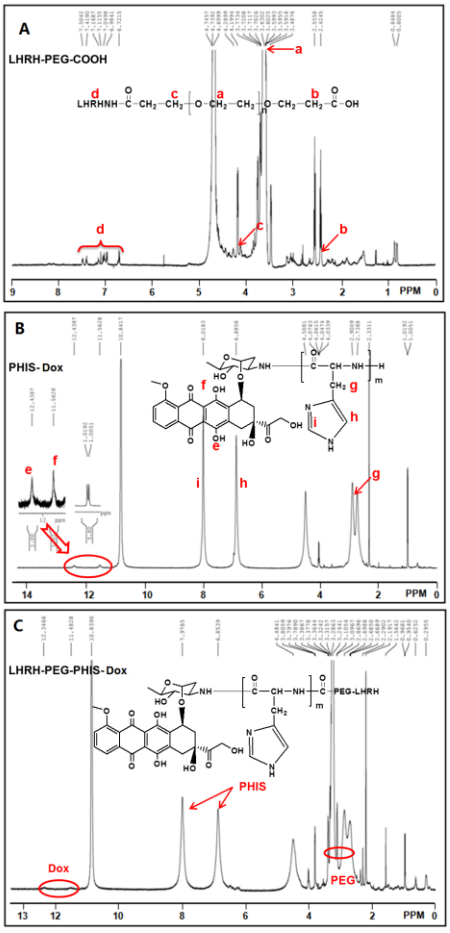

Fig. 3 ^{1}H-NMR spectra of LHRH-PEG-COOH, PHIS-Dox and LHRH-PEG-PHIS-Dox.

The molecular weight of synthesized polymer was shown in Table 1, which further confirmed the structure of the three polymers. The Dox content in the PHIS-Dox or LHRH-PEG-PHIS-Dox conjugate were 2.8 wt% and 2.1wt%, respectively.

Table 1 The molecular weights of polymers at pH 7.4.

Sample name	M_w	M_n	PDI
PHIS-DOX	18813	15548	1.21
LHRH-PEG-COOH	8556	6200	1.38
LHRH-PEG-HIS-Dox	23738	21580	1.10

M_w: Weight-average molecular weight; M_n: Number-average molecular weight;
PDI: index of polydispersity

The pK_b of imidazole in LHRH-PEG-PHIS-Dox was estimated via classical acid-base titration for defining its ionization patterns. The pK_b, critical micellar concentrations (CMC), and particle sizes at pH 7.4 were represented in Table 2. LHRH-PEG-PHIS-Dox had an inflexion point around pH 7.0 (pK_b), which was lower than that of LHRH-PEG-PHIS (pH 7.3). The pK_b shift of the LHRH-PEG-PHIS mostly resulted from increased hydration of the hydrophilic PEG and LHRH incorporation.[27] But after the hydrophobic Dox was introduced to the PHIS segments, the hydration of LHRH-PEG-PHIS-Dox reduced and resulted in a lower pK_b.

Table 2 The pK_b value, critical micellar concentrations (CMC), and particle size of polymers at pH 7.4.

Sample name	pk_b	CMC (μg/mL)	Particle size (nm)
PHIS	6.5		
LHRH-PEG- PHIS	7.3	10.0	78.2±1.5
LHRH-PEG- PHIS -Dox	7.0	4.9	85.0±2.0

To monitor micelle formation of block copolymers in phosphate buffered saline (pH 7.4, ionic strength: 0.15), pyrene was used as a fluorescence probe because it strongly illuminates in a non-polar environment and shows weak fluorescence intensity while in polar environment. The CMC, defined as the threshold concentration of self-aggregation of polymeric amphiphile by intra- and/or intermolecular association, can be determined by measuring the intensity ratio (I_{383}/I_{373}) of the third and the first highest energy bands in the emission spectra of pyrene. Figure 4 showed the intensity ratios (I_{383}/I_{373}) of LHRH-PEG-PHIS-Dox polymers as a function of concentration. The obtained CMC was 4.9 μg/mL. The lower CMC value for LHRH-PEG-PHIS-Dox compared with LHRH-PEG-PHIS (10 μg/mL) was considered by the increase of hydrophobic moiety. And this lower value indicates that LHRH-PEG-PHIS-Dox polymeric micelles are more stable in diluted media at pH 7.4.

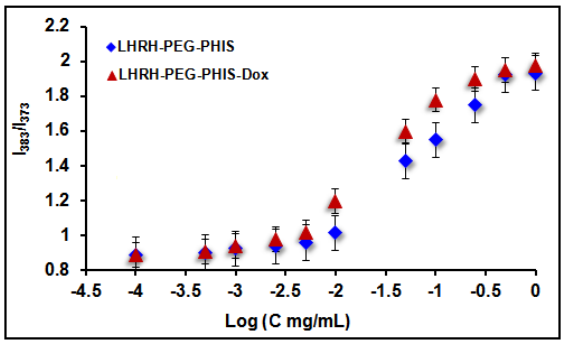

Fig. 4 The change of intensity ratio (I_{383}/I_{373}) versus the concentration of polymer values.

Preparation and characterization of LHRH-PEG-PHIS-Dox micelles

The self-assembled micelles were prepared using a modified dialysis method, which produced small particles with a narrow size-distribution. LHRH-PEG-PHIS-Dox was first dissolved in DMF, and then adding trace water to the solution. The yield of micelles was over 90%. It has been shown that by adding small amount of water directly to the organic phase prior to dialysis, micelles with a more reproducible and narrower size-distribution could be obtained.[28] The addition of some water to the organic phase appears to kinetically "freeze" the micelles, leading to a more reproducible size profile.

How to improve the drug loading efficiency is now an urgent issue in the development of drug delivery systems. This is because the drug loading efficiency was generally not more than 10% in nanoparticles or liposomes.[29,30] Here, the hydrophobic drug molecules (Dox) were chemically bonded with polymer chains (PHIS segment) as a common hydrophobic part, and combined with the hydrophilic groups to form micelles by self-assembly (Figure 5A). This simple design not only improved the stability of the micelles, but also increased the drug concentration. Dox-TAT was employed as a drug model, which was highly permeable to drug-resistant cells and greatly enhanced the cytotoxicity. Based on the equations, the

encapsulation and loading efficiencies (LE) of LHRH-PEG-PHIS-Dox/Dox-TAT micelles were 87.5wt% and 28.0wt%, respectively. And the LE of LHRH-PEG-PHIS-Dox/Dox micelles prepared was 27.8%.

The variation of the size distribution and zeta-potential were measured by Malvern Zetasizer as a function of pH. The diameter of the nanoparticles increased from 78 nm to 152 nm when the pH value decreased from 8.0 to 5.0 (Figure 5B). The size in aqueous solution was dependent on pH, likely due to the different protonation states of the PHIS segment as a function of pH. When pH was lowered to 6.0, the histidine moieties may be more ionized, and thus the charge density of aggregates increased (Figure 5C). The electrostatic repulsion between histidine moieties induced the aggregate swelling. In addition, drug-loaded micelles were larger than the blank micelles, which implied that the encapsulated Dox-TAT contributed to the enlargement of the particle size. Dox-TAT was positively charged, which may enhance the electrostatic repulsion, and then promoting the core swelling. The morphologies of micelles were observed at different pH by TEM. The obtained micelles showed a spherical geometry and a uniform appearance (Figure 5D, E, F). But their morphologies could not be maintained for 1 hour at pH 6.0 (Figure 5G). This result also showed that the micelles at slightly acidic pH values were disrupted as a result of the alternation of internal structures by imidazole ionization in the histidine moieties.

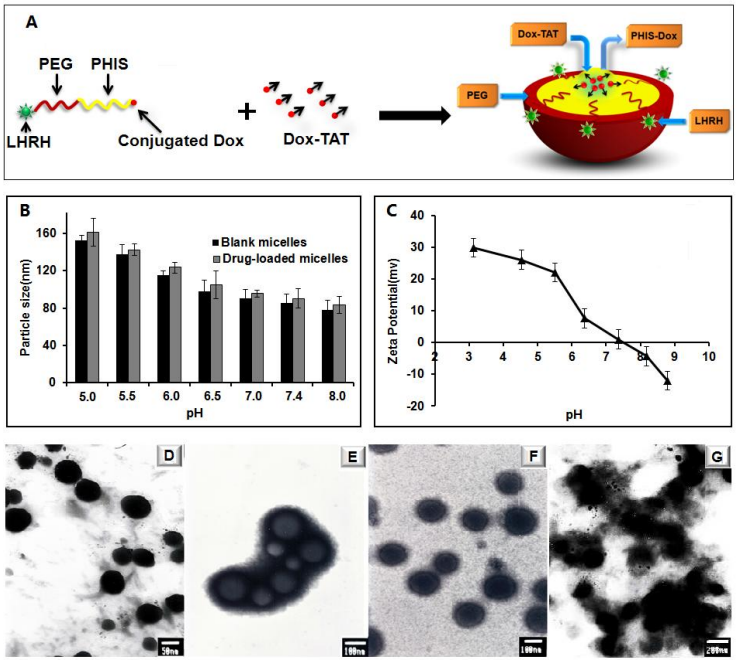

Fig. 5 (A)The formation of the LHRH-PEG-PHIS-Dox/Dox-TAT micelles. Particle size distribution of blank micelles and drug-loaded micelles at different pH(B) and zeta-potential charges (C). TEM images of LHRH-PEG-PHIS-Dox micelles at different pH (D pH7.4; E pH 6.0; F pH 5.0) and TEM image of dissociated micelles (G).

In vitro drug release studies

Figure 6A showed the *in vitro* pH-dependent release behaviors of Dox-TAT loaded LHRH-PEG-PHIS-Dox micelles in three different pH buffer solutions (pH 5.0, 6.8 and 7.4). It occurred more rapidly at either pH 5.0 or pH 6.8 buffer solution than that at pH 7.4. After 20 h, the accumulated release rate of the LHRH-PEG-PHIS-Dox micelles in pH 5.0 was 84%, while in pH 7.4 it was less than 19%. This pH sensitivity was obviously attributed to the imidazole groups of the PHIS segment. It is known that the release rate of a drug incorporated in a hydrophobic domain depends on the solubility and diffusivity of the drug.[24] However, studies of stimuli-sensitive nanoparticles have demonstrated that the drug release rate could be altered rapidly via the deformation of the inner core induced by changes in environmental conditions. Therefore, pH-triggered release from LHRH-PEG-PHIS-Dox may be consistent with pH-induced structural changes. The ionized imidazole at lower pH values may induce interior structural changes of the LHRH-PEG-PHIS-Dox micelle, and accelerate drug release rate at pH value below 7.0. During the drug release process, encapsulated Dox-TAT should be firstly released, and then the conjugated Dox should be released by amide hydrolysis. Especially at acidic pH, the accumulated release rate of Dox was very fast, which was attributed to the enhanced electrostatic repulsion between Dox-TAT and LHRH-PEG-PHIS-Dox system. In addition, the previous results have shown that chemically conjugated Dox might provide a more favorable partitioning environment for physical entrapment of Dox-TAT within the core of micelles.[31] It has been reported that the π-π interaction (non-covalent interaction between organic compounds containing aromatic rings) between the planar anthraycline ring structures of Dox molecules would be in favor of the dimerization of Dox molecules. Thus, it is likely that the conjugated Dox in LHRH-PEG-PHIS-Dox system would interact and stabilize the physically entrapped Dox-TAT.

In vitro cytotoxicity

The cytotoxic activity of drug loaded micelles was determined using MTT assay after 48 h incubation of formulation with A2780/Dox^R cells. The *in vitro* cytotoxicity at different pH displayed the pH-dependent cytotoxic effects (Figure 6B). At pH 7.4, LHRH-PEG-PHIS-Dox/Dox-TAT, LHRH-PEG-PHIS-Dox/Dox and LHRH-PEG-PHIS-Dox presented a slight cytotoxic effect against A2780/Dox^R cells. And no significant differences were noted in the cytotoxicity when compared these three groups with Dox (n=4, p>0.05). While at pH 6.8, LHRH-PEG-PHIS-Dox/Dox-TAT group showed much higher cytotoxicity (25% viability) than that of the other three groups, namely, LHRH-PEG-PHIS-Dox/Dox group (74% viability), LHRH-PEG-PHIS-Dox group (72% viability) and free Dox group (93% viability), even the concentration of LHRH-PEG-PHIS-Dox/Dox-TAT (3.8 μg/mL of Dox) was lower than that of the other three groups (14.7 μg/mL of Dox). These results may be attributed to that the released Dox-TAT from LHRH-PEG-PHIS-Dox/Dox-TAT micelles at pH 6.8 could be directly transported to the cytosol regardless of drug-resistant tumor cell lines. This was also confirmed by the effect of Dox-TAT group, in which the cell viability was significantly decreased no matter at pH7.4 (19% viability) or pH6.8 (16% viability). LHRH-PEG-PHIS micelle without drug did not show cytotoxicity under the same conditions up to a concentration of 100 μg/mL (data not shown).

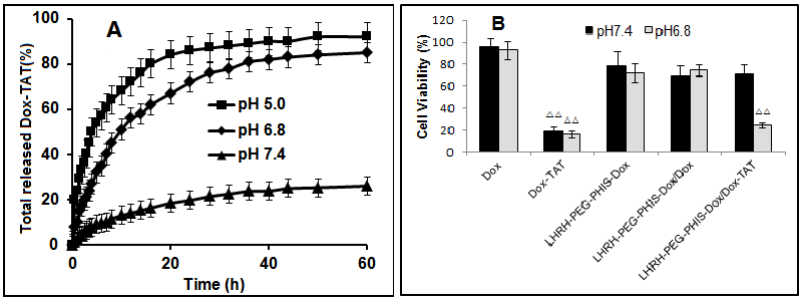

Fig.6 (A)Release profiles of Dox-TAT from LHRH-PEG-PHIS-Dox micelles at different pH at 37 ℃. (B) Relative cell viability of A2780/Dox^R cells after incubation with LHRH-PEG-PHIS-Dox/Dox-TAT, LHRH-PEG-PHIS-Dox/Dox, LHRH-PEG-PHIS-Dox, Dox-TAT or free Dox for 48h at pH 7.4 or pH 6.8. Data are shown as mean ± SD ($^{\triangle\triangle}P < 0.01$ *vs* Dox, n = 4).

Flow cytometry and cellular uptake study

The flow cytometry profiles of A2780/Dox^R cells incubated for 1 h with LHRH-PEG-PHIS-Dox/Dox-TAT, LHRH-PEG-PHIS-Dox/Dox or LHRH-PEG-PHIS-Dox micelles were shown in Figure 7. The amount of samples internalized by the cells was proportional to the fluorescence intensity of Dox (as a fluorescent marker). The cellular uptake was higher in LHRH-PEG-PHIS-Dox/Dox-TAT micelles than that of the other two groups at pH 7.4 or 6.8, which could be attributed to the TAT mediated transport. Cells incubated at pH 6.8 showed greater fluorescence in comparison with A2780/Dox^R cells incubated at pH7.4, which could be attributed to PHIS segments protonation and the micelles were at the dissociated state. Therefore, this suggested that Dox in LHRH-PEG-PHIS-Dox/Dox-TAT system can be transported into A2780/Dox^R cells by two pathways, namely, LHRH receptor-mediated endocytosis and TAT-mediated nonendocytotic process (Figure 1). In addition, LHRH-PEG-PHIS-Dox was positively charged at pH 6.8, which would promote the cellular internalization.[31] At pH 7.4, little difference was observed in the cellular uptake of Dox when A2780/Dox^R cells were incubated with LHRH-PEG-PHIS-Dox/Dox or LHRH-PEG-PHIS-Dox, which is consistent with the cytotoxicity results.

In order to confirm the drug transport process, fluorescence microscopy was performed by incubating A2780/Dox^R cells at 37 ℃ or 4 ℃. The cell culture medium was previously adjusted to pH 6.8. At 37 ℃, Dox fluorescence was shown in cytoplasm as well as nucleus (blue) when incubated with LHRH-PEG-PHIS-Dox/Dox-TAT (Figure 7I), and was significantly increased than that of LHRH-PEG-PHIS-Dox (Figure 7J). While at 4 ℃, red fluorescence was still showed in the perinuclear region and cytoplasm in LHRH-PEG-PHIS-Dox/Dox-TAT (Figure 7K), but almost no red fluorescence was shown in cells incubated with LHRH-PEG-PHIS-Dox, only the blue fluorescence (nuleus) was shown in Figure 7L. Since receptor-mediated endocytosis is an energy dependent process and could be blocked at 4 ℃,[32,33] this results confirmed that Dox in LHRH-PEG-PHIS-Dox/Dox-TAT system could be transported into A2780/Dox^R cells by two pathways, i.e. LHRH receptor-mediated endocytosis and TAT-mediated nonendocytotic process. And the LHRH-PEG-PHIS-Dox system could transport drugs within cells only by LHRH-receptor-mediated endocytosis pathway. After being endocytosed, the fusogenic activity of PHIS segments could disrupt the endosomes membrane, thus resulting in drugs reaching the cytosol to enhance the delivery efficiency. And Dox-TAT conjugate was insensitive to P-glycoprotein effux pump,[14] which also could enhance the drug delivery efficiency and overcome drug resistance through a "bypass" mechanism. These results suggested that LHRH-PEG-PHIS-Dox/Dox-TAT may be a promising delivery system to enhance Dox intracellular delivery and target the TAT peptide to tumor cells.

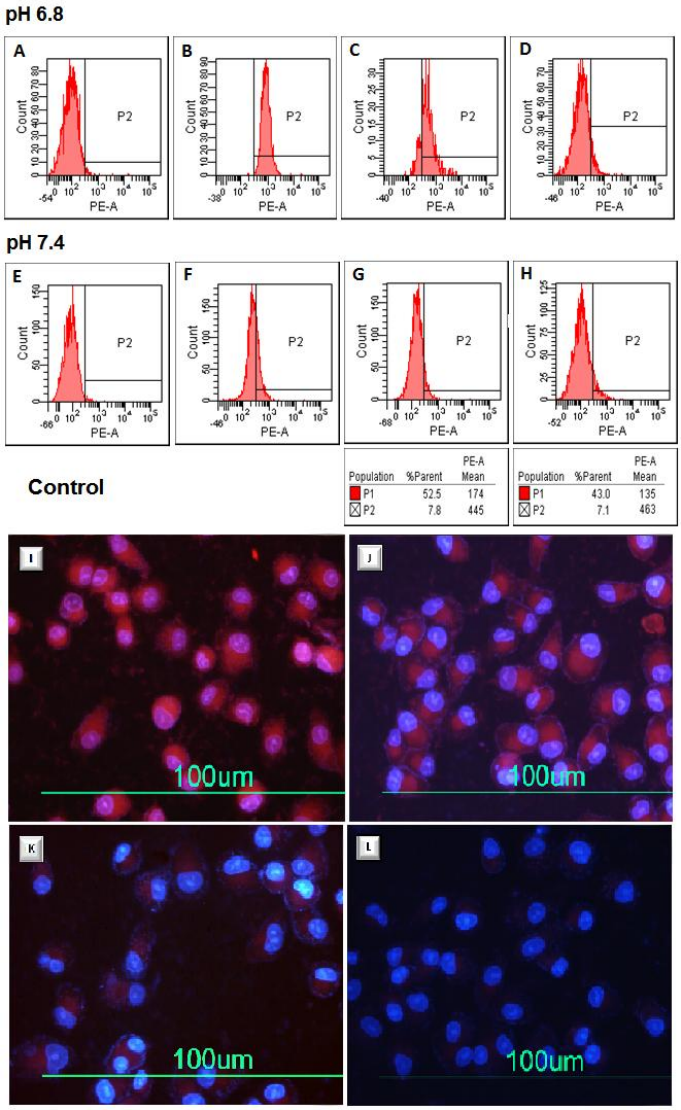

Fig. 7 FACS analysis of A2780/Dox^R cells incubated for 1 h at 37 ℃ with untreated cell as control (A,E), LHRH-PEG-PHIS-Dox/Dox-TAT(B, F), LHRH-PEG-PHIS-Dox/Dox (C, G) and LHRH-PEG-PHIS-Dox(D, H) at pH 7.4 or pH 6.8, respectively. Confocal laser scanning microscopy of A2780/Dox^R cells incubated with LHRH-PEG-PHIS-Dox/Dox-TAT (I, K) and LHRH-PEG-PHIS-Dox (J, L) micelles for 1h at 37 ℃ (I, J) or 4 ℃ (K, L), respectively.

Anti-tumor activity in vivo

The anti-tumor efficacy of LHRH-PEG-PHIS-Dox/Dox-TAT was compared with free Dox in tumor bearing nude mice and the inhibition of tumor growth was assessed via measuring the mean tumor volume (mm^3). No mice died during the experiments. The anti-tumor studies showed that LHRH-PEG-PHIS-Dox/Dox-TAT showed significantly higher efficacy in reducing the tumor volume than free Dox ($P < 0.01$) as well as LHRH-PEG-PHIS-Dox formulation ($P < 0.01$) (Figure 8A). This further confirmed that Dox in LHRH-PEG-PHIS-Dox/Dox-TAT system could be transported into A2780/Dox^R cells by two pathways as mentioned above. The possible drug transport process was as the following. The leaky vasculature of tumor tissue allows entry and retention of macromolecular architectures leading to EPR effect along with both receptor and TAT-mediated uptake. Concurrent measurement of body weight changes revealed that the LHRH-PEG-PHIS-Dox/Dox-TAT micelles showed fewer body weight shifts in comparison with group treated with plain Dox solution (Figure 8B). This significant reduction in tumor volume is clearly suggesting the biocompatibility, reduced toxicity with potential anticancer activity of LHRH-PEG-PHIS-Dox/Dox-TAT micelles in comparison with free Dox.

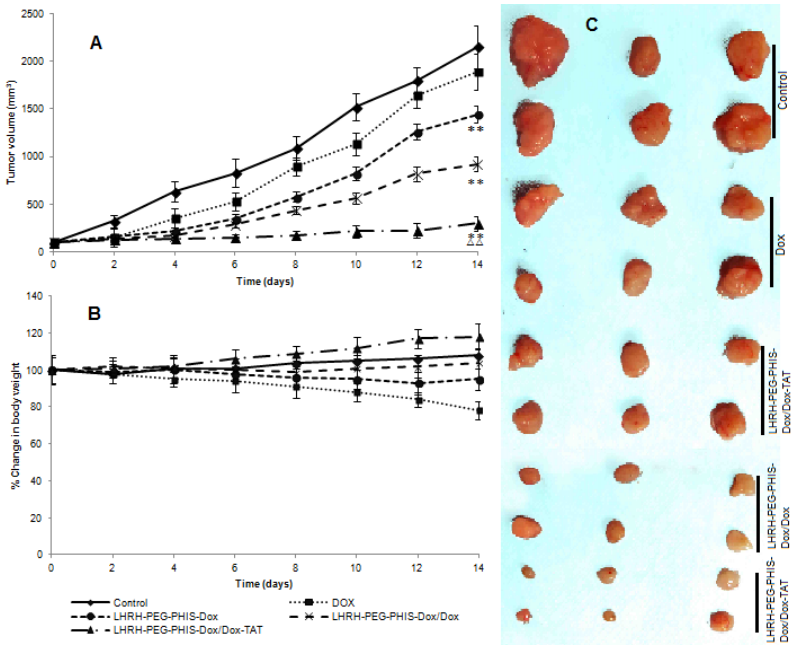

Fig. 8 (A) In vivo antitumor efficacy of micelles against A2780/Dox^R tumor. Data are shown as mean ± SD (**$P < 0.01$ *vs* control, $^{\triangle\triangle}P < 0.01$ *vs* Dox, n = 6). (B) % Body weight changes of Balb/c nuce mice bearing A2780/Dox^R tumor. Data are shown as mean ± SD (n = 6). (C) Images of tumors in tumor-bearing mice on day 14 after inoculation of tumor cells.

Conclusion

In this research, multifunctional pH-sensitive micelles LHRH-PEG-PHIS-Dox were prepared for delivering Dox-TAT, in which nonspecific TAT peptide could be protected in a simple method. Moreover, the stability of LHRH-PEG-PHIS-Dox micelles was improved through hydrophobic Dox bound to the polymer backbone (LHRH-PEG-PHIS). The micelles could dissociate responding tumor extracellular pH_e and release Dox-TAT. It occurred more rapidly at either pH 5.0 or pH 6.8 than that at pH 7.4. The released Dox-TAT could be directly transported into cytosol by the TAT mediated pathway. And the undissociated micelles could also be actively internalized into the cells by a LHRH receptor-mediated endocytosis process. These pathways resulted in enhanced cytotoxicity against LHRH-positive A2780/Dox^R cells. These results demonstrated that LHRH-PEG-PHIS-Dox/Dox-TAT micelles could combine advantages of targeted delivery and TAT peptide mediated endocytosis, while avoiding tedious procedures of chemical synthesis for shielding/deshielding of TAT peptide. This skillfully designed system combined the double effect of targeted delivery and TAT-mediated efficient entry. It may hold great potential in the development of pH-sensitive drug delivery system for drug resistant cancer cells.

Acknowledgments

This work was financially supported by the National Nature Science Foundation of China (Grant Nos 30970788 and 81271687).

References

1 Q. Leng, L. Goldgeier, J. Zhu, P. Cambell, N. Ambulos and A. J. Mixson, *Drug News Perspect.*, 2007, **20**, 77-86.
2 R. A. Petros, P. A. Ropp and J. M. DeSimone, *J. Am. Chem. Soc.*, 2008, **130**, 5008-5009.
3 M. Zorko and U. Langel, *Adv. Drug Deliv. Rev.*, 2005, **57**, 529-545.
4 E. L. Snyder and S. F. Dowdy, *Pharm. Res.*, 2004, **2**, 389-393.
5 J. S. Wadia and S. F. Dowdy, Adv. *Drug Deliv. Rev.*, 2005, **57**, 579-596.
6 M. J. Gait, *Cell. Mo. Life Sci.*, 2003, **60**, 844-853.
7 M. Rizzuti, M. Nizzardo, C. Zanetta, A. Ramirez, S. Corti, *Drug Discov. Today*, 2014, doi: 10.1016/j.drudis.2014.09.017.
8 E. L. Snyder, C. C. Saenz, C. Denicourt, B. R. Meade, X. S. Cui, I. M. Kaplan and S. F. Dowdy, *Cancer Res.*, 2005, **65**, 10646-10650.
9 S. E. Perea, O. Reyes, Y. Puchades, O. Mendoza, N. S. Vispo, I. Torrens, A. Santos, R. Silva, B. Acevedo, E. López, V. Falcón and D. F. Alonso, *Cancer Res.*, 2004, **64**, 7127-7129.
10 D. M. Theisen, C. Pongratz, K. Wiegmann, F. Rivero, O. Krut and M. Krönke, *Vaccine*, 2006, **24**, 3127-3136.

11 L. Cao, J. Si, W. Wang, X. Zhao, X. Yuan, H. Zhu, X. Wu, J. Zhu and G. Shen, *Mol. Cells*, 2006, **21**, 104-111.

12 B. Fang, L. Jiang, M. Zhang and F. Z. Ren, *Biochimie.*, 2013, **95**, 251-257.

13 J. J. Turner, G. D. Ivanova, B. Verbeure, D. Williams, A. A. Arzumanov, S. Abes, S. Abes, B. Lebleu and M. J. Gait, *Nucleic Acids Res.*, 2005, **33**, 6837-6849.

14 J. F. Liang and V. C. Yang, Bioorg. *Med. Chem. Lett*., 2005, **15**, 5071-5075.

15 V. A. Sethuraman and Y. H. Bae, *J. Control. Release*, 2007, **118**, 216-224.

16 E. S. Lee, Z. G. Gao, D. Kim, K. Park, I. C. Kwon and Y. H. Bae, *J. Control. Release*, 2008, **129**, 228-236.

17 Z. Tyrrell, Y. Shen and M. Radosz, *Prog. Polym. Sci*., 2010, **35**, 1128-1143.

18 N.Q. Shi, X.R. Qi, B. Xiang, Y. Zhang, J. Control. Release, 2014, **194**, 53-70.

19 E. S. Lee, Z. G. Gao and Y. H. Bae, *J. Control. Release*, 2008, **132**, 164-170.

20 H. Huang, Y. Li, Z.Sa, Y. Sun, Y. Wang, J. Wang, *Macromol. Biosci.*, 2014, **14**: 485-90.

21 H. Wu, L. Zhu, V. P. Torchilin, *Biomaterials*, 2013, **34**, 1213-1222.

22 L. Qiu, M. Qiao, Q. Chen, C. Tian, M. Long, M. Wang, Z. Li, W. Hu, G. Li, L. Cheng, L. Cheng, H. Hu, X. Zhao, D. Chen. *Biomaterials*, 2014, **35**: 9877-9887.

23 A.A. Kale and VP Torchilin, *J. Liposom. Res.*, 2007, **17**, 197-203.

24 M. A. Phillips, M. L. Gran and N. A. Peppas, *Nano Today*, 2010, **5**, 143-159.

25 D. Kim, E. S. Lee, K. T. Oh, Z. Gao and Y. H. Bae, *Small*, 2008, **4**, 2043-2050.

26 E. S. Lee, K. Na and, Y. H. Bae, *J. Control. Release*, 2003, **91**, 103-113.

27 D. W. Urry, S. Peng, D. C. Gowda, T. M. Parker and R. D. Harris, *Chem. Phys. Lett*., 1994, **225**, 97-103.

28 T. Lammers, W. E. Hennink and G. Storm, *Brit. J. Cancer*, 2008, 99, 392-397.

29 S. R. Yang, H. J. Lee and J.D. Kim, *J. Control. Release*, 2006, **114**, 60-68.

30 P. Xu, E. A. Van Kirk, Y. Zhan, W. J. Murdoch, M. Radosz and Y. Shen, *Angew. Chem. Int. Ed. Engl.*, 2007, **46**, 4999-5002.

31 A. Nori, K. D. Jensen, M. Tijerina, P. Kopeckova and J. Kopecek, *Bioconju. Chem.*, 2003, **14**, 44-50.

32 K. T. Oh, E. S. Lee, D. Kim and Y. H. Bae, *Int. J. Pharm.*, 2008, **358**, 177-183.

33 J. Lin, J. Zhu, T. Chen, S. Lin, C. Cai, L. Zhang, Y. Zhuang and X. S. Wang, *Biomaterials*, 2009, **30**, 108-117.